

Special Section: Organic Materials Used in Agriculture, Horticulture, Reconstructed Soils, and Filtering Applications



Maps of soil water availability for plants are a tool for precision irrigation management, allowing the growers to save water and apply an accurate amount of water in appropriate areas.

Jonathan A. Lafond, Silvio J. Gumiere, Dennis W. Hallema, Yann Périard, and Jean Caron, Département des sols et de génie agroalimentaire, Université Laval, 2480 boul. Hochelaga, Québec, QC, Canada, G1V 0A6; Sylvain Jutras, Département des sciences du bois et de la forêt, Université Laval, 2405 rue de la Terrasse, Québec, QC, Canada, G1V 0A6. *Corresponding author (jonathan.lafond.2@ulaval.ca).

Vadose Zone J.
doi:10.2136/vzj2014.10.0140
Received 7 Oct. 2014.
Accepted 31 Jan. 2015.

© Soil Science Society of America
5585 Guilford Rd., Madison, WI 53711 USA.

All rights reserved. No part of this periodical may be reproduced or transmitted in any form or by any means, electronic or mechanical, including photocopying, recording, or any information storage and retrieval system, without permission in writing from the publisher.

Spatial Distribution Patterns of Soil Water Availability as a Tool for Precision Irrigation Management in Histosols: Characterization and Spatial Interpolation

Jonathan A. Lafond,* Silvio J. Gumiere, Dennis W. Hallema, Yann Périard, Sylvain Jutras, and Jean Caron

Lettuce (*Lactuca sativa* L.) production in organic soils is important in Quebec, Canada. Lettuce is highly sensitive to tip burn, a physiological disorder that can lead to significant yield losses. Tip burn losses have been linked to various factors, such as root water uptake deficits. A precision irrigation approach using local applications of water based on lettuce requirements and soil water available capacity (SWAC) reduces the occurrence of tip burn but may need mapped spatial information of SWAC for proper irrigation management. The objectives of this study were (i) to determine a rapid, efficient, and reliable method for interpolating SWAC and (ii) to use this interpolation method in precision irrigation simulations in management zones to demonstrate the importance of using SWAC maps. The methods for SWAC interpolation used in this study were inverse distance weighting (IDW), thin plate splines (TPS) and kriging with external drift (KED). The simulation used a calculation procedure for mass balance that contained SWAC maps, evapotranspiration (ET) and precipitation. A comparison of each interpolation method and multiple statistical criteria revealed that IDW and KED were the most precise methods, depending on the study site. Simulations of precision irrigation showed that in many cases, local irrigation management in seven to eight zones must account for the spatial distribution of SWAC to attain an 80% irrigation adequacy for lettuce. Hence, using SWAC maps as a tool for managing irrigation would allow growers to save water and to apply an accurate amount of water in appropriate areas.

Abbreviations: ET, evapotranspiration; IDW, inverse distance weighting; KED, kriging with external drift; SWAC, soil water available capacity; TPS, thin plate splines.

Lettuce is an important crop produced in Canada, particularly in Quebec (an average of 58,092 t was produced annually between 2008 and 2011; MAPAQ and ISQ, 2012). Approximately 2800 ha of Quebec land, mostly Histosols, are used for lettuce production each year. In the United States, lettuce production represent about 278,900 acres and 90 million cwt of lettuce, with 53 million cwt head lettuce, 26 million cwt of Romaine lettuce and 11 million cwt of leaf lettuce (Lu et al., 2011; Mossler and Dunn, 2014). In 2002, lettuce production on muck soil in Florida represented about 1% of US lettuce (head, leaf, or Romaine lettuce). These organic soils are known to have specific properties that modulate water storage and movement in the root zone layers (Schlotzhauer and Price, 1999; Brandyk et al., 2002; Lafond et al., 2014). Moreover, organic deposits are often spatially heterogeneous, as the nature of the material may vary dramatically both horizontally and with depth (Heathwaite and Göttlich, 1993). Hence, these variations can influence irrigation management practices (Périard et al., 2012). An understanding of the spatial variability in the soil water storage capacity at the field scale is therefore crucially important to improving irrigation management and saving water and energy.

Soil water available capacity is a simple and widely used concept that defines the amount of water that the soil can hold, which can be used by plants to grow. Generally, the maximum available water capacity is the difference between the soil water content at field capacity and the soil water content at the permanent wilting point of a specific crop (Romano and Santini, 2002). Since Veihmeyer and Hendrickson (1927) first described water availability, many authors have refined the concept to yield more realistic estimates and to obtain a more universal and comprehensive definition (Letey, 1985; Da Silva et al., 1994; Groenevelt et al., 2001; Minasny and McBratney, 2003). Caution should be taken when considering a simple estimation of available water capacity because it is a static or semistatic concept (Romano and Santini, 2002). Water fluxes and transpiration rates in the soil–plant–atmosphere system should be accounted for by using numerical models, which provide a superior evaluation of available water for plants compared with observations alone. Estimates of available water capacity for plants are easiest to obtain and apply (e.g., in mapping and irrigation management) in well-defined situations for a specific crop in a specific soil.

Mapping of available water for plants requires interpolation of measured spatial data. Inverse distance weighting (IDW), thin plate splines (TPS) and kriging, which are the most commonly used methods in hydrological and soil properties interpolations, are used in this study (Ahmed and De Marsily, 1987; Cooke et al., 1993). The IDW method is based on an inverse weighting function of distance between data points in which the weights depend on an exponent that must be greater than zero (Webster and Oliver, 2007). For instance, a value of 2 indicates that interpolation points are calculated based on surrounding data points weighted by their squared distances. The IDW method is deterministic and is not discontinuous when the weighting exponent is greater than zero (Webster and Oliver, 2007). However, the choice of the weighting exponent is somewhat arbitrary, and the IDW method does not consider the configuration of the sampling scheme (Webster and Oliver, 2007). On the other hand, TPS is a deterministic method with a local stochastic component; it is also a continuous interpolator, but it provides the option of either interpolating at the exact data points or estimating points that produce a smoother surface (Webster and Oliver, 2007). Thin plate splines may be compared to bending a thin sheet of metal to match the measured data. This method can be characterized by local accuracy and global accuracy. The optimization of the interpolation is performed by using an objective function that involves minimizing (i) the error between the observations and interpolated values at the observation locations and (ii) the bending of the thin metal sheet. The minimum error at the observation locations maximizes the local accuracy, while minimizing the bending energy of the sheet detracts from the local accuracy, and increases the global accuracy. An advantage of the TPS method over kriging is its simplicity (Boer et al., 2001). Kriging is a stochastic approach in which a trend and its residual components can be modeled by a semivariogram (Webster

and Oliver, 2007). The residual components represent the realizations of the zero mean and the uncorrelated random errors, and these residuals are modeled through a parametric function of the semivariance for various distances between data points. Kriging estimations are continuous, local, and either linear or nonlinear, and they follow a wide range of least-squares methods for spatial estimations (Webster and Oliver, 2007). An evaluation of the differences between the spatial interpolation methods is the first step in spatially characterizing the soil water available capacity as a tool for precision irrigation.

The objectives of this study were to (i) compare the different interpolators and determine a rapid, efficient, and reliable method for interpolating soil water available capacity and (ii) use this interpolation method in a simulation of precision irrigation in several management zones to investigate the scale of irrigation subunits for optimizing water use and to demonstrate the importance of SWAC maps as a tool for precision irrigation.

Materials and Methods

Study Area and Soil Characteristics

This study was conducted on cultivated organic soils near Sherrington (45°13' N, 73°52' W), southwestern Quebec, Canada, from 2009 to 2012. These Histosols can mainly be classified as Haplohemists (Soil Survey Staff, 1999), which have been used for agriculture for more than 50 yr. The major crop is lettuce, but onion (*Allium cepa* L.), carrot (*Daucus carota* L.), and celery (*Apium graveolens* L.), among other crops, are also produced in large quantities. The study area comprises five farms that cover approximately 1880 ha of organic soils: Production Horticole van Winden (PHVW; 45.1328°N, 73.5252°W; ~155 ha), Les Fermes Hotte et van Winden Inc. (HVW; 45.1337°N, 73.4467°W; ~185 ha), Maraîchers JPL Guérin et Fils Inc. (JPG; 45.1577°N, 73.6231°W; ~145 ha), Vert Nature Inc. (VN; 45.1274°N, 73.5189°W; ~1020 ha), and Delfland Inc. (DELF; 45.1962°N, 73.3583°W; approximately 375 ha). At the five farms, a total of 207 geo-referenced soil profiles (Fig. 1) were selected to collect samples,

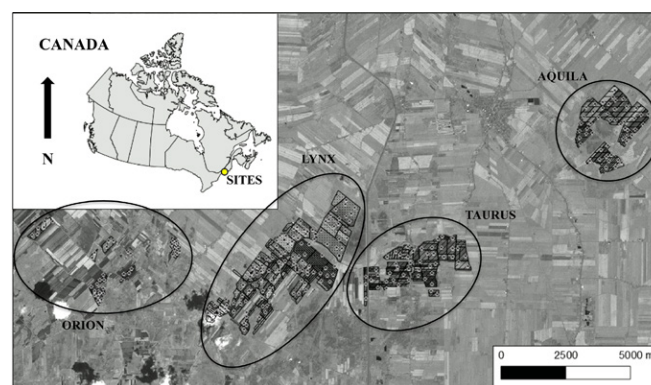


Fig. 1. Spatial distribution of the sampling soil profiles ($n = 207$) over the four sites (AQUILA, LYNX, TAURUS, and ORION).

which were characterized and analyzed for soil physical properties (see next section). Spatial data for the five farms were divided into four sites (spatial regions): AQUILA, LYNX, TAURUS, and ORION (Fig. 1).

Measurements of Soil Physical Properties in the Laboratory

First, each soil profile was examined to distinguish the horizon types and thicknesses according to the Canadian System of Soil Classification (Soil Classification Working Group, 1998) and to record the total depth of the organic profile, that is, the thickness of the organic soil above the mineral substrate. Second, 5.50-cm-high and 8.25-cm-diameter cores were sampled at four depths (5–10, 20–25, 35–40, and 50–55 cm), stored in plastic bags (in pieces) and transported to the laboratory to measure the soil bulk density (Blake and Hartge, 1986), total organic content (Karam, 1993), and total porosity (Parent and Caron, 1993). Finally, undisturbed cores (5.50-cm height \times 8.25-cm diameter) were collected in the same manner but at two depths (SU: \sim 20 cm; PR: \sim 35 cm) and transported intact to the laboratory to characterize the saturated hydraulic conductivity (Reynolds and Elrick, 2002), soil water retention curve (Dane and Hopmans, 2002; Romano et al., 2002), and unsaturated hydraulic conductivity when possible (Hopmans et al., 2002).

Modeling Soil Water Retention Curves

After obtaining the water retention curves, we estimated the parameters of the van Genuchten (1980) water retention model and two variations of the Groenevelt and Grant (2004) model for each of the 207 samples: the first model relies on the vegetation-specific wilting point for Romaine lettuce (-300 cm; Périard et al., 2012), and the second model relies on the soil water saturation point and the vegetation-specific temporary wilting point for Romaine lettuce. For these models, the lowest RMSE was chosen for determining the water content at matric potentials corresponding to the thresholds for the SWAC calculations (see next section). Soil water retention curve modeling was performed using R (R Development Core Team, 2012). A complete cluster analysis of the water retention curves for the same studied sites is presented and discussed in details by Hallema et al. (2015). Experimental data of water retention were obtained either from a tension table (Romano et al., 2002) or from a pressure cell device (Dane and Hopmans, 2002), but both methods were considered, giving comparable results. Verification of this assumption was performed using some duplicate cores (results not shown). The main difference between the methods is that the first method only reached a matric potential of -200 cm, while the pressure cells sometimes reached -500 cm of matric potential. Therefore, values at -300 cm often had to be estimated from the best fit model.

SWAC Calculations

Calculations of soil water available capacity (SWAC; cm) were performed by considering the plant–soil system of Romaine lettuce

growth in organic soils. Lettuce has a root penetration depth up to 1 m where the organic soil profile is not too compacted (Plamondon-Duchesneau, 2011). Therefore, the maximum depth in the SWAC calculation was fixed at 1 m. The soil thickness for the storage capacity was further divided into two layers: (i) a surface horizon, which is often compacted and decomposed, and (ii) a deeper horizon, which is often mesic or fibric and less decomposed. Equation [1] expresses the calculation of SWAC:

$$SWAC_i = \int_{z_0}^{z_1} [\theta_{fc}(SU_i) - \theta_{twp}] dz_1 + \int_{z_1}^{z_2 \leq 100} [\theta_{fc}(PR_i) - \theta_{twp}] dz_2 \quad [1]$$

where i is a given soil profile, z_0 is the soil surface, z_1 is the depth of the first layer (cm), z_2 is the depth of the soil profile (cm) up to 100 cm, θ_{fc} is the water content at field capacity ($\text{cm}^3 \text{cm}^{-3}$), θ_{twp} is the water content at the temporary wilting point ($\text{cm}^3 \text{cm}^{-3}$), SU_i is the surface horizon's undisturbed core of the i th soil profile, and PR_i is the deeper horizon's undisturbed core of the i th soil profile. Based on previous studies on the same soil (Périard et al., 2012), the field capacity of the surface horizon (often Oh or Ohp) was fixed at a corresponding matric potential of -50 cm and that of a deeper horizon (often Om or Of) was fixed at -25 cm. The temporary wilting point for Romaine lettuce was determined at a matric potential of -300 cm. Effectively, the classical definition of soil water available for plants considers the difference between water content values at the field capacity and permanent wilting point (Romano and Santini, 2002). However, for agronomic reasons associated with cultivating lettuce in organic soils (i.e., irrigation, growing cycle, lettuce disorders as tip burn), soil water “readily” available for plants was considered as the difference between the field capacity and temporary wilting point of lettuce.

The saturated hydraulic conductivity (K_{sat} , cm s^{-1}) was also necessary for the SWAC calculations. Notably, the first horizon of these organic soil profiles is sometimes conducive to limiting water infiltration, due to a compacted layer, and causing a perched water table at the interface of the deeper horizon (Lafond et al., 2014). The depth where this compacted layer may be present was sampled for undisturbed cores (named SU). Subsequently, the K_{sat} of these SU cores was measured in the laboratory. A water velocity on the order of $10^{-4} \text{ cm s}^{-1}$ was found to limit adequate infiltration of the perched water table (personal observations). Therefore, for a soil profile with this type of limiting situation, the SWAC could not be calculated over the entire soil profile. Equation [2] was used instead of Eq. [1] for this specific situation:

$$SWAC_i = \int_{z_0}^{z_1} [\theta_{fc}(SU_i) - \theta_{twp}] dz_1 \quad [2]$$

Note that in this situation, roots have difficulty penetrating the hardened layer. As a result, the capacity for water uptake may decrease and asphyxia may occur near the perched water table. Therefore, locations with limiting K_{sat} values are critical when considering irrigation management strategies.

Spatial Interpolation Methods

Three spatial interpolation methods were evaluated: IDW, TPS, and KED. In the IDW method, the weight given to an observation is inversely associated with its distance to the prediction location. The predicted value $\hat{Z}(x_0)$ at an arbitrary nonmeasured location x_0 can be obtained by (Bivand et al., 2013):

$$\hat{Z}(x_0) = \frac{\sum_{i=1}^n w(x_i) Z(x_i)}{\sum_{i=1}^n w(x_i)} \quad [3]$$

where $w(x_i)$ is the weight associated with the observation at location x_i and $Z(x_i)$ is the observation at location x_i . The relationship between weight and distance is calculated by the power law of the distance between x_i and x_0 :

$$w(x_i) = \frac{1}{d(x_i - x_0)^p} \quad [4]$$

where d is the distance and p is a power that determines how quickly the weight decreases with distance; a greater value of p adds more weight to the closest observations. In this study, three different values of p were used (0.5, 2, and 4). The IDW method is called an exact interpolator, when the prediction location coincides with an observation location and the associated weight is infinite; consequently, the prediction at that location is equal to the observed value.

The splines interpolation method consists of fitting a series of polynomials to the observations. The thin plate splines interpolation method (TPS) is equivalent to the two-dimensional cubic splines first developed by Wahba (1990). In the TPS method, the value $Z(x_i)$ at location x_i is calculated as (Boer et al., 2001):

$$Z(x_i) = f(x_i) + \varepsilon(x_i) \quad [5]$$

where f is an unknown smoothing function, $\varepsilon(x_i)$ is random error and $i = 1, \dots, n$ indicates the dataset vector. The function f is estimated by minimizing:

$$\sum_{i=1}^n [\hat{Z}(x_i) - f(x_i)]^2 + \lambda J_2(f) \quad [6]$$

where λ is the smoothing parameter estimated by a cross-validation. The measure of smoothness of f , $J_2(f)$ is calculated by integrating the biharmonic function in two dimensions $\nabla^4(x, y)$:

$$J_2(f) = \iint \left[\left(\frac{\partial^2 f}{\partial x^2} \right)^2 + \left(\frac{\partial^2 f}{\partial x \partial y} \right)^2 + \left(\frac{\partial^2 f}{\partial y^2} \right)^2 \right] dx dy \quad [7]$$

In this study, we used the TPS function from the fields package (Nychka et al., 2014) to perform the TPS interpolation. The TPS procedure in the fields package includes a cross-validation

subroutine for surface optimization over the dataset. However, to compare the interpolation methods, the performance of TPS was estimated using the same cross-validation procedure that was used for the other two interpolation methods.

Kriging is a generic name for a group of interpolation techniques for data that present spatial associations (Schuenemeyer and Drew, 2010). In this study, only universal kriging, which is also referred to as kriging with external drift (KED), is tested. Kriging can be considered a type of auto-regression in which the residuals are spatially correlated and the relative distance of the neighboring data points are accounted for during the interpolation procedure. The interpolated surface defined by kriging passes through the measured data points when a predicted point lies at the exact location of an observed value. The kriging estimator is defined by:

$$\hat{Z}(x) - m(x) = \sum_{i=1}^n \lambda_i [Z(x_i) - m(x_i)] \quad [8]$$

where $m(x)$ and $m(x_i)$ are the expected values of $Z(x)$ and $Z(x_i)$ and, respectively, λ_i is the weight assigned to the point $Z(x_i)$, and λ_i is estimated by minimizing the error variance:

$$\sigma_E^2(x) = \text{Var}[\hat{Z}(s) - Z(s)] \quad [9]$$

Subject to the constraint $E[\hat{Z}(x) - Z(x)] = 0$, the estimation of the weight parameter requires a function for the covariance between $\hat{Z}(x)$ or $Z(x)$ and distance, which is given by the semivariogram model:

$$\gamma \equiv \frac{1}{2|N(b)|} \sum_{N(b)} [Z(x_i) - Z(x_i + b)]^2 \quad [10]$$

where γ is the semi-variance, N is the number of pairs, and b is the distance between pairs of points.

In this study, we used the automatic-fitting kriging routine from the R package automap (Hiemstra et al., 2009), based on the gstat package (Pebesma, 2004). The fitting routine uses least-squares fitting to identify an optimal fit between the semivariogram model and the sample semivariogram.

Evaluation of the Goodness of Fit

The performance of the five spatial interpolation methods was determined with a leave-one-out cross-validation procedure. We used the following criteria to evaluate the cross-validation performance: the mean error (ME), mean absolute error (MAE), root mean square error (RMSE), and standard deviation of error (SDE). These criteria were chosen because they reflect different evaluations of each interpolation method based on the cross-validation procedure. Table 1 shows the evaluation criteria and their respective ranges.

Results and Discussion

Evaluation of Soil Water Availability for Lettuce

The mean values of soil water availability at each site (13.7 cm over all sites; Table 2) were generally comparable to those reported in the literature (Hanna et al., 1982). The mean values ranged from 11.7 to 16.9 cm for the LYNX and AQUILA sites, respectively; the LYNX site presented the most decomposed profiles, while the AQUILA site presented the least decomposed profiles. Note that SWAC is influenced by soil water content and total porosity (Ritchie, 1981), which is related to the degree of decomposition in organic soils (Brandyk et al., 2002). Over the four sites, thickness of the organic soil profile was ranging from 20 to 260 cm, bulk density varied from 0.132 to 0.562 g cm⁻³, total organic content ranged between 42.6 and 96.7%, total porosity between 0.706 and 0.912 cm³ cm⁻³, and saturated hydraulic conductivity between 1.14×10^{-5} and 6.32×10^{-2} cm s⁻¹. These ranges indicated a wide variety of organic soil profile and degree of decomposition over the four sites, which will impact on SWAC.

The highest value of the SWAC was approximately 30 cm (ranging from 28.2 to 34.3 cm; Table 2), which is realistic for organic soils or peat materials where more than 50% of the water retention occurs between matric potentials of -1 and -10 kPa (Heiskanen, 1995). The standard deviations varied between 4.5 and 6.9 cm, while the coefficients of variation were small (between 0.3 and 0.6; Table 2), reflecting a homogeneous repartition of the SWAC values over the mean. However, these indicators of the SWAC variance do not necessarily reflect the spatial heterogeneity of the SWAC distribution patterns.

Comparison of the Spatial Interpolation Methods

Table 3 and Fig. 2 presents the goodness of fit for the three spatial interpolation methods of the SWAC at each of the four sites (AQUILA, LYNX, TAURUS, and ORION), while Fig. 3 to 6 (a-e) present the SWAC maps at each site (for each of the interpolation methods). The RMSE and MAE criteria provide a measure of the interpolation accuracy, while the SDE criteria is a measure of the interpolation precision, all with lower values (near zero) indicating more accurate or precise methods. The ME measures the bias (Hosseini et al., 1994). Here, the RMSE indicator was chosen over the MAE to discuss the superior interpolation method. The best RMSE (4.557 cm; Table 3) was obtained at the AQUILA site with the IDW method using a power p value of 0.5 (Fig. 2c and 3a). However, at the same AQUILA site, much smaller bias was obtained using the KED method (ME = -0.01058 cm; Table 3 and Fig. 2a) than the IDW- $p = 0.5$ method (ME = -0.1021; Table 3 and Fig. 2a), probably accounting for less smoothing using the KED method (Fig. 3d) than the IDW- $p = 0.5$ method (Fig. 3a). The most precise interpolation method at the AQUILA site was also the IDW- $p = 0.5$ method, followed by the KED method (SDE =

Table 1. Criteria used for evaluating the goodness of fit.

Criterion†	Equation	Range
ME	$ME = \frac{1}{n} \sum_{i=1}^n (\hat{Z}_{cv,i} - Z_i)$	$[-\infty, \infty]$ best = 0
MAE	$MAE = \frac{1}{n} \sum_{i=1}^n \hat{Z}_{cv,i} - Z_i $	$[0, \infty]$ best = 0
RMSE	$RMSE = \sqrt{\frac{1}{n} \sum_{i=1}^n (\hat{Z}_{cv,i} - Z_i)^2}$	$[0, \infty]$ best = 0
SDE	$SDE = \sqrt{\frac{\sum_{i=1}^n (\hat{Z}_{cv,i} - Z_i)^2}{n-1}}$	$[0, \infty]$ best = 0
† ME, mean error; MAE, mean absolute error; RMSE, root mean squared error; SDE, standard deviation of error.		

Table 2. Descriptive statistics of the soil water available capacity (SWAC) presented for each site and for the total over all sites.

Descriptive statistics	Total SWAC	By site			
		AQUILA	LYNX	TAURUS	ORION
	cm				
<i>n</i>	207	45	91	37	34
Min.	2.0	9.3	2.0	2.9	2.0
Max.	34.3	28.2	33.0	28.6	34.3
Mean	13.7	16.9	11.7	14.1	14.7
Median	13.5	17.1	10.5	13.3	14.1
SD	6.5	4.5	6.9	6.1	6.3
CV	0.5	0.3	0.6	0.4	0.4

Table 3. Goodness of fit for the spatial interpolation of the soil water available capacity (cm) at each sector (AQUILA, LYNX, TAURUS, and ORION).

Site	Methods†	ME‡	MAE	RMSE	SDE
AQUILA	IDW $p = 0.5$	-0.1021	3.673	4.557	4.607
	IDW $p = 2$	-0.3244	3.94	4.844	4.888
	IDW $p = 4$	-0.4051	4.291	5.263	5.306
	TPS	-0.0259	3.729	4.645	4.697
	KED	-0.01058	3.876	4.726	4.780
LYNX	IDW $p = 0.5$	0.00993	5.457	6.879	6.917
	IDW $p = 2$	0.0733	5.01	6.443	6.478
	IDW $p = 4$	0.2417	5.072	6.452	6.483
	TPS	0.004912	4.927	6.591	6.627
	KED	0.1248	4.728	6.187	6.220
TAURUS	IDW $p = 0.5$	-0.02276	4.886	6.039	6.123
	IDW $p = 2$	-0.04037	4.144	5.237	5.309
	IDW $p = 4$	0.006672	3.859	5.239	5.312
	TPS	0.4549	4.294	5.826	5.888
	KED	0.02762	4.172	5.293	5.366
ORION	IDW $p = 0.5$	0.01353	4.522	6.581	6.680
	IDW $p = 2$	0.2395	4.963	7.217	7.321
	IDW $p = 4$	0.5587	5.448	7.965	8.064
	TPS	-0.2991	4.931	7.558	7.666
	KED	1.36×10^{-14}	4.494	6.432	6.529

† IDW, inverse distance weighting; TPS, thin plate splines; KED, kriging with external drift.

‡ ME, mean error; MAE, mean absolute error; RMSE, root mean squared error; SDE, standard deviation of error.

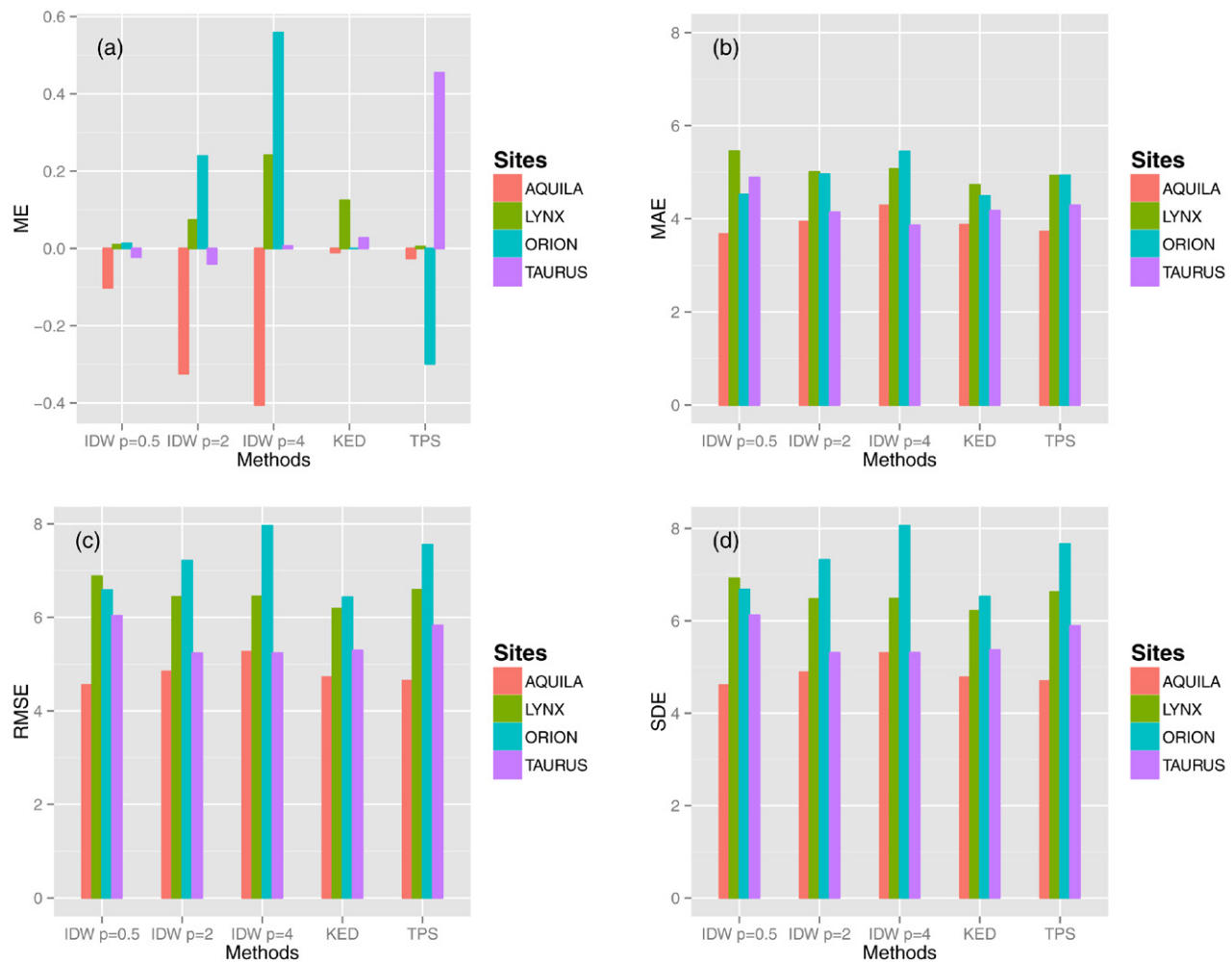


Fig. 2. Comparison of the interpolation methods (IDW- $p = 0.5$, IDW- $p = 2$, IDW- $p = 4$, KED, and TPS) at each site (AQUILA, LYNX, TAURUS, and ORION) for each of the goodness of fit indicator: (a) ME, mean error; (b) MAE, mean absolute error; (c) RMSE, root mean squared error; and (d) SDE, standard deviation of error.

4.607; Table 3 and Fig. 2d). At the ORION and LYNX sites, KED was more accurate, with RMSEs of 6.432 and 6.187 cm (Table 3, Fig. 2c, 4d, and 6d). Precision of the KED method led to the same result for these two sites with SDEs of 6.529 and 6.220 cm (Table 3, Fig. 2d). However, at the LYNX site, the TPS method produced very small bias compared with the KED method ($ME = 4.912 \times 10^{-3}$ cm vs. 0.1248 cm; Table 3 and Fig. 2a). This result suggests that the TPS method would have less biased SWAC values at the x locations compared with the KED method, but it would also provide less accurate and precise estimates than the KED method. We chose to use the accuracy indicator (RMSE) instead of the bias indicator (ME) for selecting the best interpolation method at the ORION and LYNX sites (the KED method). At the TAURUS site, the best interpolation accuracy and precision were obtained with the IDW- $p = 2$ method, with an RMSE of 5.237 cm and a SDE of 5.309 cm (Table 3 and Fig. 2c and 2d). However, very small bias was obtained using the IDW- $p = 4$ method ($ME = 6.672 \times 10^{-3}$ cm vs. -4.037×10^{-2} cm for IDW- $p = 2$; Table 3 and Fig.

2a). At the TAURUS site, the IDW- $p = 4$ method produced an RMSE of 5.239 cm, which was much closer to the IDW- $p = 2$ method (a 0.002 difference). Moreover, the IDW- $p = 4$ method at this site produced a better MAE estimation than the IDW- $p = 2$ method (3.859 cm and 4.144 cm, respectively; Table 3 and Fig. 2b). Considering these results, the IDW- $p = 4$ method was considering superior for obtaining a reliable SWAC map at the TAURUS site (Fig. 5c). Overall, the best spatial interpolations were obtained with the IDW (AQUILA and TAURUS) and KED (ORION and LYNX) methods, depending on the site (Table 3; Fig. 2). This information should now be used as a tool for precision irrigation.

Local Management of Irrigation—Simulation and Analysis

In the context of irrigation management, an irrigation map must consider the influence of spatial heterogeneities by accounting for the realistic lettuce growing cycle. Hence, we used the hydrological balance method based on the cumulative potential

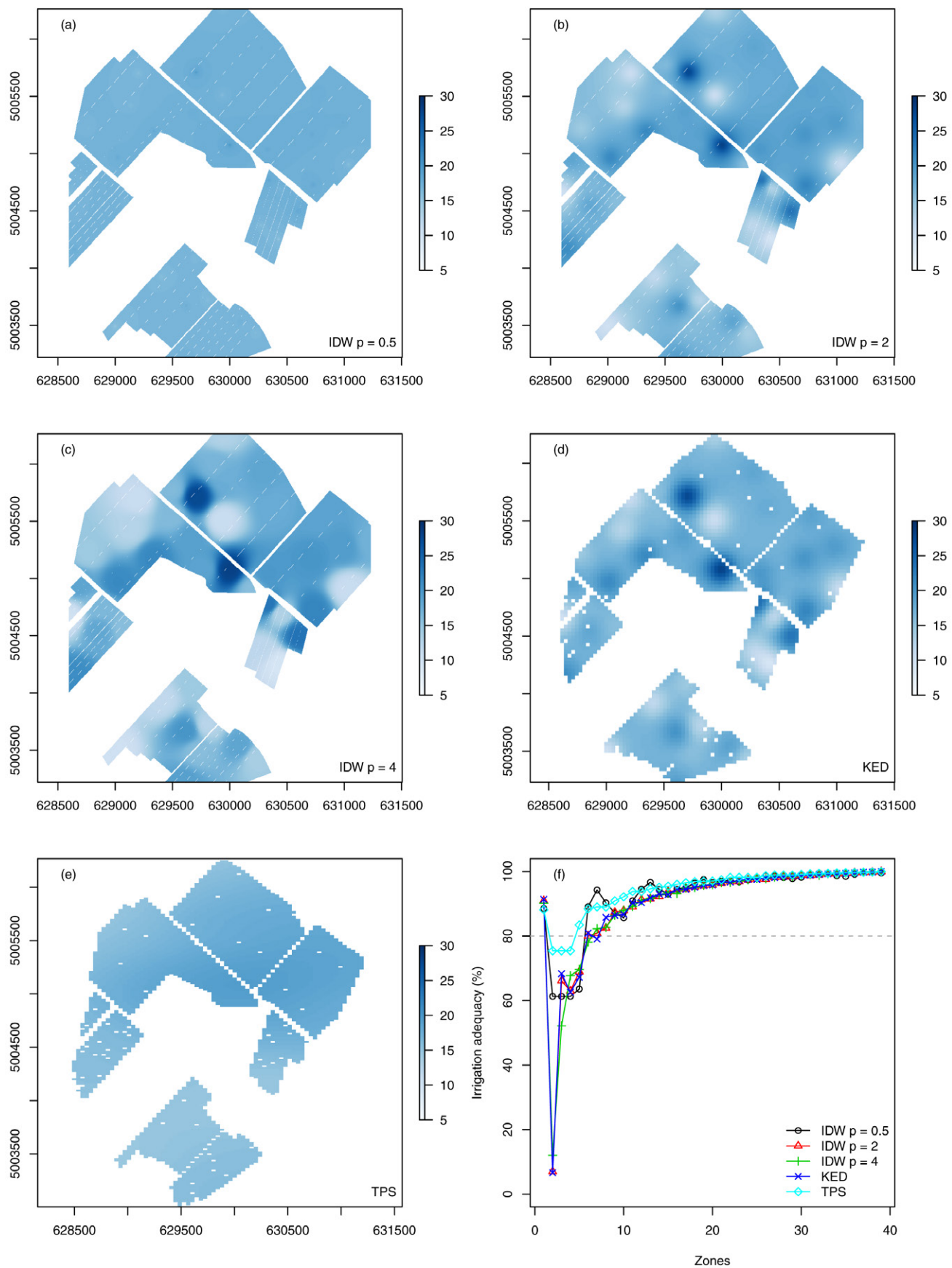


Fig. 3. Soil water available capacity (SWAC) maps at the AQUILA site for each interpolation method: (a) IDW- $p = 0.5$, (b) IDW- $p = 2$, (c) IDW- $p = 4$, (d) KED, and (e) TPS, followed by (f) the results of the simulation analysis reporting the adequacy of irrigation (%) to supply the lettuce needs by considering the SWAC maps as a function of the number of irrigation management zones.

evapotranspiration over a growing period of Romaine lettuce (~ 45 d) to calculate the irrigation amount required for the evaporative demand by considering the SWAC. We decided to simulate scenarios of irrigation management based on SWAC maps with 1 to 40 local management zones for each spatial interpolation method and each site, which corresponded to managing irrigation from an entire farm scale (350–450 ha) to field units (1–10 ha). At the AQUILA site, at least 80% of the irrigation adequacy was attained with only one zone ($\sim 90\%$; Fig. 3f), regardless of the interpolation method employed. This one zone system consisted in managing irrigation according to the mean SWAC. However, this simulation also showed that if one chose to manage the AQUILA site within two to five irrigation zones, the adequacy of irrigation to supply the lettuce needs, according to the SWAC, would drop below 60% using most interpolation methods. At higher number of irrigation units (5 irrigation zones and more), the adequacy gradually increases logarithmically up to almost 100% at 40 management zones. Notably, at more than 15 zones in this case, the gain reach in adequacy of irrigation to supply the lettuce needs, according to the SWAC, would be small ($\sim 5\%$). This result is advantageous from a practical point of view because the irrigation could be managed with only one uniform zone that reflects the average SWAC over the site (Fig. 7a); the costs of employees, irrigation material, and measurement equipment would be reduced compared with a highly heterogeneous area.

Figure 4 shows the SWAC maps for the LYNX site. Based on the RMSE values presented in Table 3, the best interpolation method was KED (Fig. 4d). The LYNX site presents more spatial heterogeneity in the SWAC distribution patterns, where some locations require less irrigation than others. To reach this arbitrary threshold of 80% of irrigation adequacy, the site must be divided into eight or more zones (Fig. 4f). Similarly to the AQUILA site, increasing the number of irrigation management zones at the LYNX site has an asymptotic log relationship with the irrigation adequacy (Fig. 3f and 4f). Over eight zones, the increase in the adequacy of irrigation to supply the lettuce needs, according to the SWAC, was gradual. However unlike the AQUILA site, the LYNX site did not have a one-zone peak irrigation adequacy over 80%, suggesting that growers should manage irrigation locally following a SWAC distribution patterns of at least eight zones (Fig. 7b).

At the TAURUS site, 80% of the irrigation adequacy was attained using seven zones by following the IDW- $p = 4$ interpolation method (Fig. 5f). This result is comparable to that at the LYNX site, and the relationship between the number of zones and the irrigation adequacy was also asymptotic and logarithmic. A small irrigation adequacy peak of approximately 60% was found using only one irrigation management zone, but the grower should be aware that this type of irrigation (one zone) would probably not meet water requirements for lettuce according to the SWAC map (Fig. 5c). Hence, some locations might be too dry or too wet; as a result, the lettuce may experience disorders such as tip burn

(Périard et al., 2012). Tip burn is a major problem for lettuce growers because when a field exhibits about 10% tip burn, it becomes not economically efficient to harvest the field. Périard et al. (2012) demonstrated that within 1 d, depending on the evapotranspirative demand, a lettuce field can switch from “normal” to “not harvestable” because of tip burn occurrence if it is not irrigated adequately and at the right time. Hence, such disorders may be controlled by adequate local irrigation management following the best SWAC map (Fig. 7c). The accuracy of the SWAC map is therefore essential in evaluating the adequacy of irrigation to supply the lettuce needs.

At the ORION site, the irrigation adequacy limit of 80% using the KED interpolation method (Table 3, Fig. 6d) was also attained with two irrigation management zones (Fig. 6f). This site was unique as it presents many clusters of cultivated organic soils (Fig. 1). Despite there being multiple clusters in this “constellation” (ORION site), it did not affect the RMSE negatively. Therefore, ORION may be considered as one site on the same basis as AQUILA, LYNX, and TAURUS. Then KED appeared to be a suitable method considering that a strong drift could be modeled (Fig. 6d). Interestingly, the simulation produced an irrigation adequacy at the ORION site using the KED method that was characterized by a linear-sill relationship (Fig. 6f) rather than the log relation seen at the other sites (Fig. 3f, 4f, and 5f). Hence, using the average SWAC as a tool for managing irrigation at the ORION site would be a suitable approach (Fig. 7d).

Conclusions and Perspectives

A conclusion of this study is that there is no universal spatial interpolation method for characterizing SWAC; that is, the best interpolation method is site dependent. Inverse distance weighting was the best method at the AQUILA and TAURUS sites, while KED was the most accurate interpolation method at the ORION and LYNX sites, according to the RMSE. The SWAC maps produced using each interpolation method were either homogeneous, where the average SWAC was represented, or heterogeneous. This simple finding is very important for irrigation management. The chosen interpolation method effectively appears to have a strong impact on irrigation management. Two sites (LYNX and TAURUS) require seven or eight irrigation management zones to achieve 80% irrigation adequacy. In more uniform cases, the irrigation adequacy may be achieved with as little as one or two zones. These more uniform sites can be easier to manage and are less costly in terms of farm resources. Additionally, local management may reduce water consumption and increase the adequacy of irrigation to supply the lettuce needs according to SWAC. However, economical analyses should be performed in conjunction with this study to optimize irrigation management, yields, and production expenses.

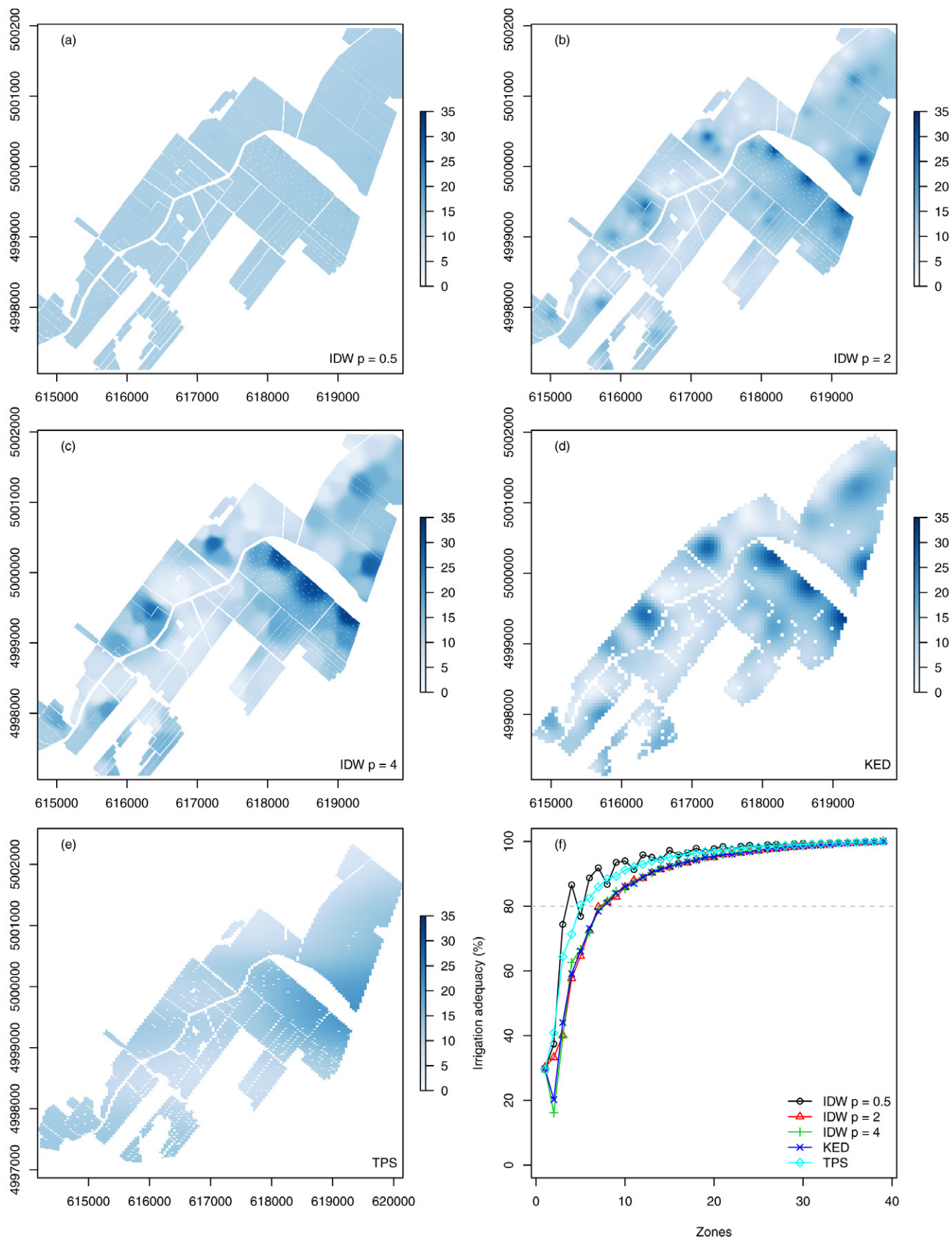


Fig. 4. Soil water available capacity (SWAC) maps at the LYNX site for each interpolation method: (a) IDW- $p = 0.5$, (b) IDW- $p = 2$, (c) IDW- $p = 4$, (d) KED, and (e) TPS, followed by (f) the results of the simulation analysis reporting the adequacy of irrigation (%) to supply the lettuce needs by considering the SWAC maps as a function of the number of irrigation management zones.

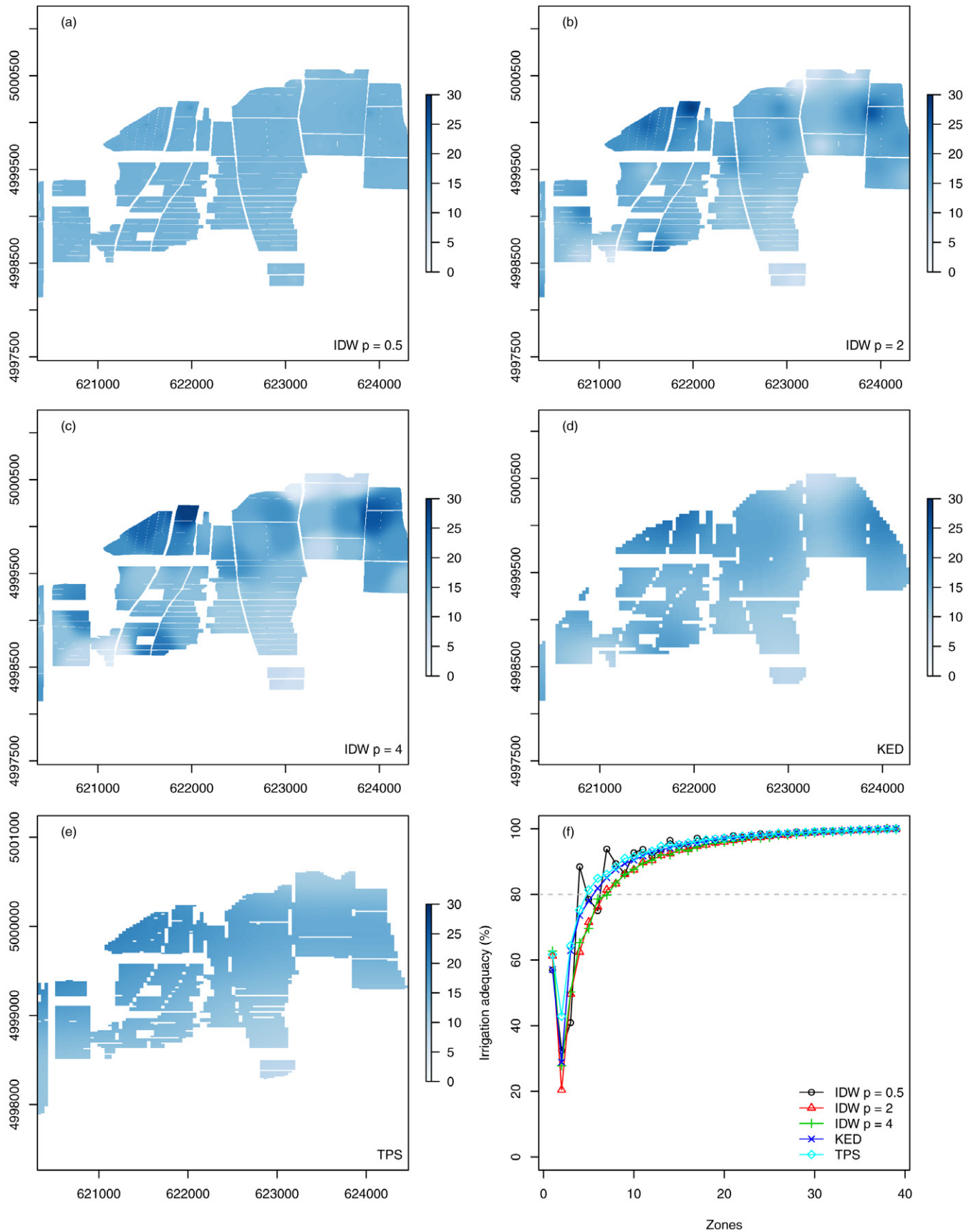


Fig. 5. Soil water available capacity (SWAC) maps at the TAURUS site for each interpolation method: (a) IDW- $p = 0.5$, (b) IDW- $p = 2$, (c) IDW- $p = 4$, (d) KED, and (e) TPS, followed by (f) the results of the simulation analysis reporting the adequacy of irrigation (%) to supply the lettuce needs by considering the SWAC maps as a function of the number of irrigation management zones.

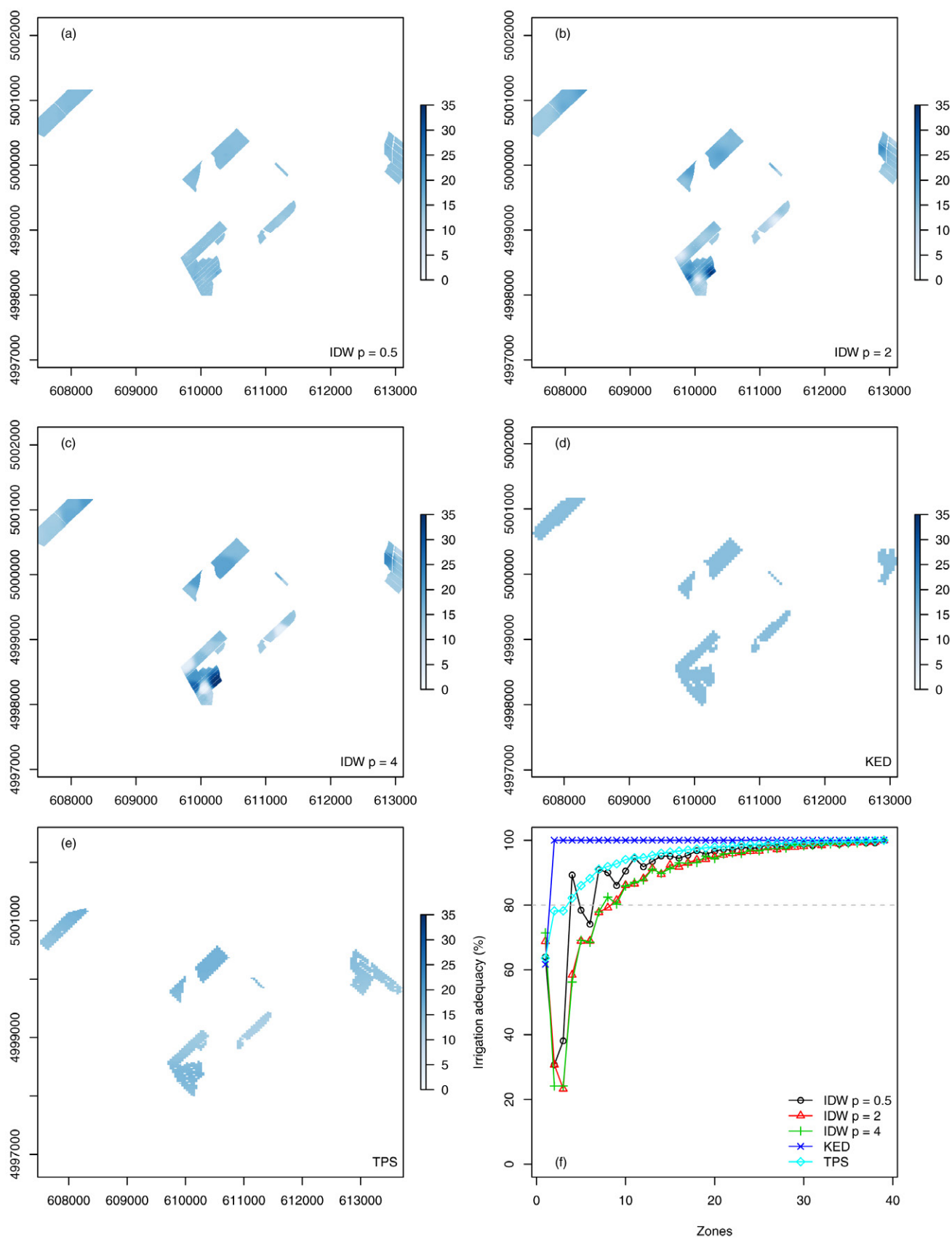


Fig. 6. Soil water available capacity (SWAC) maps at the ORION site for each interpolation method: (a) IDW- $p = 0.5$, (b) IDW- $p = 2$, (c) IDW- $p = 4$, (d) KED, and (e) TPS, followed by (f) the results of the simulation analysis reporting the adequacy of irrigation (%) to supply the lettuce needs by considering the SWAC maps as a function of the number of irrigation management zones.

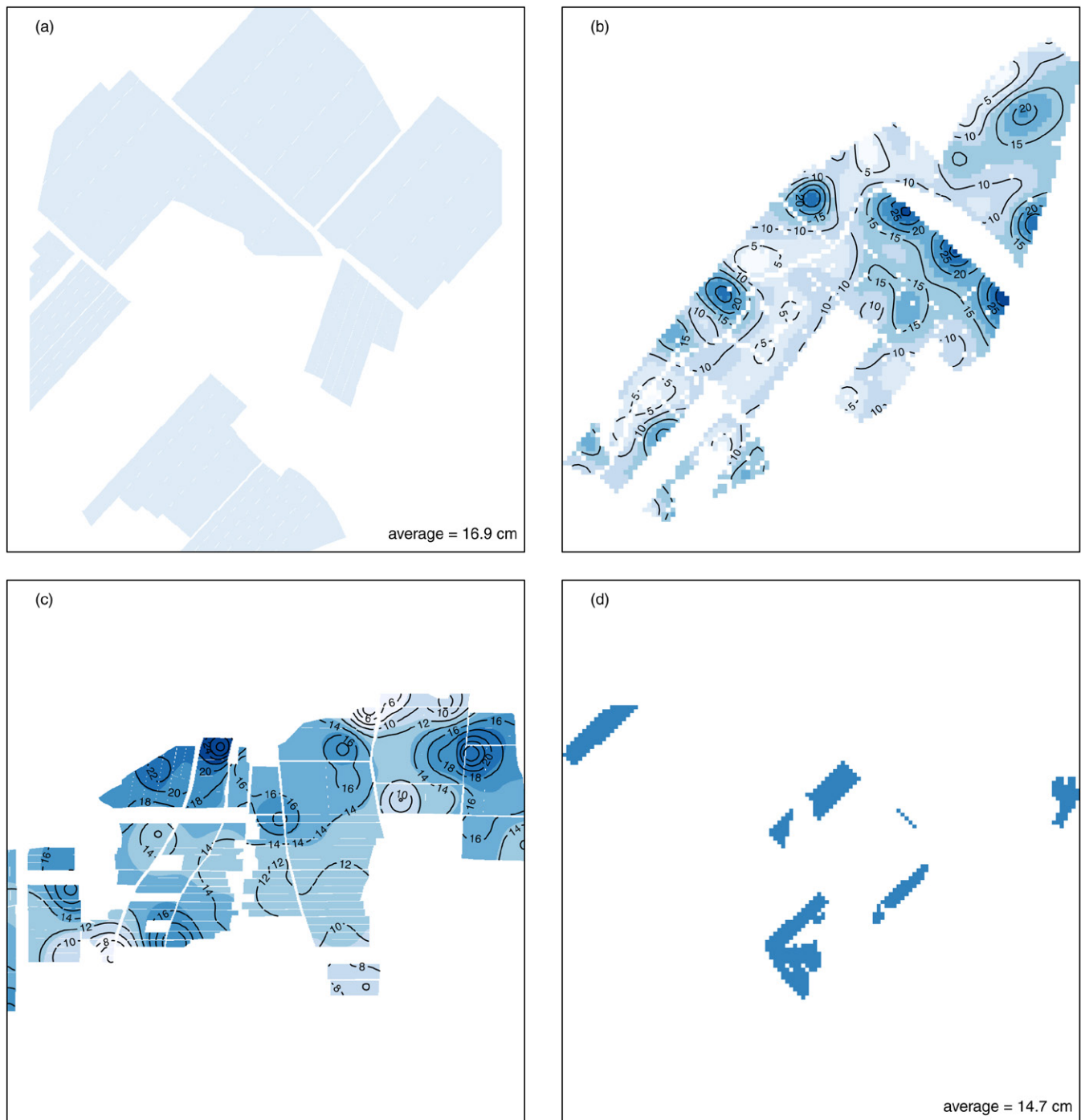


Fig. 7. Comparison of SWAC maps for each site: (a) AQUILA, (b) LYNX, (c) TAURUS, and (d) ORION, according to best method of interpolation: (a) IDW- $p = 0.5$, (b) KED, (c) IDW- $p = 4$, and (d) KED and according to the ideal number of zones of: (a) 1, (b) 8, (c) 7, and (d) 2 to reach at least 80% irrigation adequacy.

Acknowledgments

We would like to thank the undergraduate students who helped with the fieldwork. We also acknowledge the financial support of the Natural Sciences and Engineering Research Council of Canada (NSERC) through a Collaborative Research and Development Grant in partnership with Productions Horticoles Van Winden Inc., Les Fermes Hotte et Van Winden Inc., Maraichers J.P. & L. Guérin et Fils Inc., Delfland Inc., and Vert Nature Inc.

References

- Ahmed, S., and G. De Marsily. 1987. Comparison of geostatistical methods for estimating transmissivity using data on transmissivity and specific capacity. *Water Resour. Res.* 23(9):1717–1737. doi:10.1029/WR023i009p01717
- Bivand, R.S., E. Pebesma, and V. Gómez-Rubio. 2013. *Applied spatial data analysis with R*. 2nd ed. Springer, New York.
- Blake, G.R., and K.H. Hartge. 1986. Bulk density. In: A. Klute, editor, *Methods of soil analysis. Part 1. Physical and mineralogical methods*. 2nd ed.

- SSSA Book Ser. 5. ASA and SSSA, Madison, WI. p. 363–375. doi:10.2136/sssabookser5.1.2ed.c13
- Boer, E.P.J., K.M. de Beurs, and A.D. Hartkamp. 2001. Kriging and thin plate splines for mapping climate variables. *Int. J. Appl. Earth Obs. Geoinf.* 3(2):146–154. doi:10.1016/S0303-2434(01)85006-6
- Brandyk, T., J. Szatylowicz, R. Oleszczuk, and T. Gnatowski. 2002. Water-related physical attributes of organic soils. In: L.É. Parent and P. Ilnicki, editors, *Organic soils and peat materials for sustainable agriculture*. CRC Press, Boca Raton, FL. p. 33–66.
- Cooke, R.A., S. Mostaghimi, and J.B. Campbell. 1993. Assessment of methods for interpolating steady-state infiltrability. *Trans. ASAE* 36(5):1333–1341. doi:10.13031/2013.28467
- Dane, J.H., and J.W. Hopmans. 2002. Pressure cell. In: J.H. Dane and G.C. Topp, editors, *Methods of soil analysis. Part 4. Physical methods*. SSSA Book Ser. 5. SSSA, Madison, WI. p. 684–688. doi:10.2136/sssabookser5.4.c25
- Da Silva, A.P., B.D. Kay, and E. Perfect. 1994. Characterization of the least limiting water range of soils. *Soil Sci. Soc. Am. J.* 58:1775–1781. doi:10.2136/sssaj1994.03615995005800060028x
- Groenevelt, P.H., and C.D. Grant. 2004. A new model for the soil-water retention curve that solves the problem of residual water contents. *Eur. J. Soil Sci.* 55(3):479–485. doi:10.1111/j.1365-2389.2004.00617.x
- Groenevelt, P.H., C.D. Grant, and S. Semetsa. 2001. A new procedure to determine soil water availability. *Aust. J. Soil Res.* 39:577–598. doi:10.1071/SR99084
- Hallema, D.W., Y. Périard, J.A. Lafond, S.J. Gumiere, and J. Caron. 2015. Characterization of water retention curves for a series of cultivated Histosols. *Vadose Zone J.* 14 (this issue). doi:10.2136/vzj2014.10.0147
- Hanna, A.Y., P.W. Harlan, and D.T. Lewis. 1982. Soil available water as influenced by landscape position and aspect. *Agron. J.* 74:999–1004. doi:10.2134/agronj1982.00021962007400060016x
- Heathwaite, A.L., and K. Göttlich, editors. 1993. *Mires: Process, exploitation and conservation*. John Wiley and Sons, Chichester, UK.
- Heiskanen, J. 1995. Physical properties of two-component growth media based on Sphagnum peat and their implications for plant-available water and aeration. *Plant Soil* 172:45–54. doi:10.1007/BF00020858
- Hiemstra, P.H., E.J. Pebesma, C.J.W. Twenhöfel, and G.B.M. Heuvelink. 2009. Real-time automatic interpolation of ambient gamma dose rates from the Dutch radioactivity monitoring network. *Comput. Geosci.* 35(8):1711–1721. doi:10.1016/j.cageo.2008.10.011
- Hopmans, J.W., J. Šimůnek, N. Romano, and W. Durner. 2002. Inverse methods. In: J.H. Dane and G.C. Topp, editors, *Methods of soil analysis. Part 4. Physical methods*. SSSA Book Ser. 5. SSSA, Madison, WI. p. 963–1008. doi:10.2136/sssabookser5.4.c40
- Hosseini, E., J. Gallichand, and D. Marcotte. 1994. Theoretical and experimental performance of spatial interpolation methods for soil salinity analysis. *Trans. ASAE* 37(6):1799–1807. doi:10.13031/2013.28269
- Karam, A. 1993. Chemical properties of organic soils. In: M.R. Carter, editor, *Soil sampling and methods of analysis*. Canadian Society of Soil Science. Lewis Publishers, Boca Raton, FL. p. 459–472.
- Lafond, J.A., É. Bergeron Piette, J. Caron, and G. Thérioux Rancourt. 2014. Evaluating fluxes in Histosols for water management in lettuce: A comparison of mass balance, evapotranspiration and lysimeter methods. *Agric. Water Manage.* 135:73–83. doi:10.1016/j.agwat.2013.12.016
- Letey, J. 1985. Relationship between soil physical properties and crop production. *Adv. Soil Sci.* 1. Springer, New York, p. 277–294.
- Lu, H., A.L. Wright, and D. Sui. 2011. Responses of lettuce cultivars to insect pests in southern Florida. *Horttechnology* 21:773–778.
- MAPAQ and ISQ. 2012. Profil sectoriel de l'industrie horticole au Québec. Ministère de l'Alimentation du Québec and Institut de la Statistique du Québec.
- Minasny, B., and A.B. McBratney. 2003. Integral energy as a measure of soil-water availability. *Plant Soil* 249:253–262. doi:10.1023/A:1022825732324
- Mossler, M.A., and E. Dunn. 2014. Florida crop/pest management profile: Lettuce. Univ. Florida, Inst. Food and Agricultural Sciences, Gainesville.
- Nychka, D., R. Furrer, and S. Sain. 2014. *Fields: Tools for spatial data*. R package version 7.1. <http://CRAN.R-project.org/package=fields> (accessed 26 Feb. 2014).
- Parent, L.É., and J. Caron. 1993. Physical properties of organic soils. In: M.R. Carter, editor, *Soil sampling and methods of analysis*. Canadian Society of Soil Science. Lewis Publishers, Boca Raton, FL. p. 441–458.
- Pebesma, E.J. 2004. Multivariable geostatistics in S: The gstat package. *Comput. Geosci.* 30(7):683–691. doi:10.1016/j.cageo.2004.03.012
- Périard, Y., J. Caron, S. Jutras, J.A. Lafond, and A. Houliot. 2012. Irrigation management of Romaine lettuce in Histosols at two spatial scales: Water, energy, leaching and yield impacts. In: H. Bjornlund, C.A. Brebiba, and S. Wheeler, editors, *WIT Trans. Ecol. Environ.* 4th Int. Conf. Sustainable Irrig. Drain. Manage. Technol. Policies 168:171–188.
- Plamondon-Duchesneau, L. 2011. Gestion de l'irrigation des laitues romaines (*Lactuca sativa* L.) cultivées en sol organique. Département de Phytologie, Faculté des Sciences de l'Agriculture et de L'alimentation, Université Laval, Québec, Canada.
- R Development Core Team. 2012. R: A language and environment for statistical computing. R Foundation for statistical computing, Vienna, Austria.
- Reynolds, W.D., and D.E. Elrick. 2002. Constant head soil core (tank) method. In: J.H. Dane and G.C. Topp, editors, *Methods of soil analysis. Part 4. Physical methods*. SSSA Book Ser. 5. SSSA, Madison, WI. p. 804–808. doi:10.2136/sssabookser5.4.c31
- Ritchie, J.T. 1981. Soil water availability. *Plant Soil* 58:327–338. doi:10.1007/BF02180061
- Romano, N., J.W. Hopmans, and J.H. Dane. 2002. Suction table. In: J.H. Dane and G.C. Topp, editors, *Methods of soil analysis. Part 4. Physical methods*. SSSA Book Ser. 5. SSSA, Madison, WI. p. 692–698. doi:10.2136/sssabookser5.4.c25
- Romano, N., and A. Santini. 2002. Available water. In: J.H. Dane and G.C. Topp, editors, *Methods of soil analysis. Part 4. Physical methods*. SSSA Book Ser. 5. SSSA, Madison, WI. p. 731–734. doi:10.2136/sssabookser5.4.c26
- Schlotzhauer, S.M., and J.S. Price. 1999. Soil water flow dynamics in a managed cutover peat field, Quebec: Field and laboratory investigations. *Water Resour. Res.* 35(12):3675–3683. doi:10.1029/1999WR900126
- Schuenemeyer, J.H., and L.J. Drew. 2010. *Spatial Statistics In: Statistics for earth and environmental scientists*. John Wiley and Sons, Hoboken, NJ. p. 151–192.
- Soil Classification Working Group. 1998. The Canadian system of soil classification. General Direction of Research, Agriculture and Agri-Food Canada, Publ. 1646. 3rd ed. National Research Council Canada, Ottawa, ON.
- Soil Survey Staff. 1999. *Soil taxonomy: A basic system of soil classification for making and interpreting soil surveys*. 2nd ed. USDA Agric. Handb. 436. USDA-NRCS, U.S. Gov. Print. Office, Washington, DC.
- van Genuchten, M.Th. 1980. A closed-form equation for predicting the hydraulic conductivity of unsaturated soils. *Soil Sci. Soc. Am. J.* 44:892–898. doi:10.2136/sssaj1980.03615995004400050002x
- Veihmeyer, F.J., and A.H. Hendrickson. 1927. Soil-moisture conditions in relation to plant growth. *Plant Physiol.* 2(1):71–82. doi:10.1104/pp.2.1.71
- Wahba, G. 1990. *Spline models for observational data*. Society for Industrial and Applied Mathematics, Philadelphia, PA.
- Webster, R., and M.A. Oliver. 2007. *Geostatistics for environmental scientists*. 2nd ed. John Wiley and Sons, Chichester, UK.